Dentomaxillofacial Radiology (2020) 50, 20200391
© 2021 The Authors. Published by the British Institute of Radiology
birpublications.org/dmfr

RESEARCH ARTICLE

Parotid gland tumors: comparison of conventional and diffusion-weighted MRI findings with histopathological results

[1]Can Zafer Karaman, [1,2]Ahmet Tanyeri, [1,3]Recep Özgür and [1,4]Veli Süha Öztürk

[1]Department of Radiology, Aydın Adnan Menderes University School of Medicine, Aydın, Turkey; [2]Department of Radiology, Yozgat City Hospital, Yozgat, Turkey; [3]Department of Radiology, Devrek State Hospital, Zonguldak, Turkey; [4]Department of Radiology, Salihli State Hospital, Manisa, Turkey

Objectives: The aim of this study was to investigate the relationship between pathological classification of parotid gland tumors and conventional MRI – diffusion-weighted imaging findings and also contribute the possible effect of apparent diffusion coefficient (ADC) to diagnosis.
Methods: 60 patients with parotid masses diagnosed using histopathology and/or cytology were enrolled in this retrospective study. All patients were evaluated using a 1.5 T MRI. Demographic features, conventional MRI findings, and ADC values (mean, minimum, maximum, and relative) were recorded. MRI findings and ADC values were compared between benign–malignant groups and pleomorphic adenoma *vs* Warthin's tumor groups.
Results: 60 tumors (48 benign, 12 malignant) were evaluated in a total of 60 patients (39 males, 21 females). The mean age was 59 (±14, 18–86) years old; the mean lesion size was 26 (±10, 11–61) mm. On the texture of conventional MRI, T2 dominantly hyperintense/with hypointensity signal was seen in 87% of pleomorphic adenomas and T2 dominantly hypointense/with hyperintesity signal was encountered in 64% of all Warthin's tumors. Seven (28%) Warthin's tumors were misdiagnosed as pleomorphic adenomas and two others (8%) as malignant tumors. The commonly used mean ADC value was $1.6 \pm 0.6 \times 10^{-3}$ mm^2 s^{-1} for benign tumors, $0.8 \pm 0.3 \times 10^{-3}$ mm^2 s^{-1} for malign tumors, 1 (0.9–1.8) $\times 10^{-3}$ mm^2 s^{-1} for Warthin's tumors, and $1.9 \pm 0.3 \times 10^{-3}$ mm^2 s^{-1} for pleomorphic adenomas. There was a statistically significant difference in ADC values between benign-malignant tumors and pleomorphic adenomas-Warthin's tumors.
Conclusions: Warthin's tumor may occasionally be misdiagnosed as pleomorphic adenoma and malignant tumor because of variable morphologic features. In addition to benign–malignant differentiation, the added ADC measurement may also be useful for differentiating Warthin's tumors from pleomorphic adenomas.
Dentomaxillofacial Radiology (2020) **50**, 20200391. doi: 10.1259/dmfr.20200391

Cite this article as: Karaman CZ, Tanyeri A, Özgür R, Öztürk VS. Parotid gland tumors: comparison of conventional and diffusion-weighted MRI findings with histopathological results. *Dentomaxillofac Radiol* 2020; **50**: 20200391.

Keywords: Parotid gland tumors; Diffusion-weighted imaging; Apparent diffusion coefficient; Magnetic resonance imaging; Salivary gland

Introduction

Salivary gland tumors constitute of 3–12% of head and neck region tumors and 2–3% of all body tumors. It is the tissue with the largest tumor histopathological subgroup among all organs, and tumors are most frequently originated from the parotid gland.[1,2] In treatment planning and surgical method selection for parotid gland tumors, it is important to discriminate benign and malignant lesions and subgroup determination.[3] Fine needle aspiration cytology (FNAC) has been demonstrated to be a

Correspondence to: Mr Veli Süha Öztürk, E-mail: md.suhaozturk@gmail.com
Received 12 August 2020; revised 22 October 2020; accepted 19 November 2020

useful and reliable tool in the pre-operative diagnosis of parotid gland masses.[4] However, in addition to general and region-specific invasive interventional risks in FNAC, tumor cell spreading in pleomorphic adenomas and malignant lesions may lead to an increased recurrence ratio. In addition, the distinction between some benign and malignant lesions in cytological examination is not only difficult, but also sometimes impossible.[5,6]

MRI is superior to ultrasonography and CT in identifying lesions and showing the surrounding tissue interface. Although all data acquired with MRI (lesion morphology, signal intensity and contrast pattern, etc.) are combined for mass characterization, there may be overlap between neoplastic lesions.[7] Recently, there are studies reporting that ADC measurement obtained with diffusion-weighted imaging (DWI), which provides information about the microcirculation and vascular physiology of the tumor, has high potential in identifying benign–malignant tumor bias and subgroup determination.[8–12] Today, for many reasons, DWI has become a key method due to its impact on technological developments. The fast method (can be applied in one breath cycle) is a non-contrast test that can be quickly integrated into existing protocols. Despite these advantages, the use of this method in salivary gland and other head and neck tumors is still very novel and more data are needed. There are some recent sophisticated MR sequences, such as diffusion tensor imaging, intravoxel incoherent motion diffusion MR imaging, proton spectroscopy, and dynamic susceptibility contrast imaging have been used to characterize salivary gland tumors.[13] These advanced techniques are generally not applicable in routine practice, still need to be corroborated and require additional studies for their clinical application.

For all of these reasons, we aimed to determine the relationship between the histopathological results of the parotid gland tumors and the imaging findings on conventional MRI with an emphasis on T_2 weigthed sequence and DWI findings, with possible contribution of DWI to the diagnosis.

Methods and materials

Ethics committee approval was received for this study from the Adnan Menderes University Faculty of Medicine (April 24, 2017-E.24352). The cases with an MRI obtained for the salivary gland in our institution (Adnan Menderes University Faculty of Medicine Department of Radiology) between December 2009 and 2016 were analyzed retrospectively. 122 cases with parotid masses were identified. Those cases had no histopathological (surgical specimen) and/or cytological (fine needle aspiration) diagnosis, and tumors that were inconspicuous in the ADC map were excluded from the study. Tumors bigger than 1 cm were included. As a result, 60 tumors of the remaining 60 cases constituted the study group. In the presence of more than one tumor in the same gland or a similar second tumor in the contralateral gland, only the largest tumor was taken under consideration. Demographic features including age and gender were recorded.

All of the morphological features and signal characteristics of the masses were re-evaluated through the Picture Archiving and Communication System (PACS). Quantitative measurements were made on the ADC map through the image analysis software program (Myrian, Imoios, Montpellier, France). Histopathological and/or cytological diagnoses were recorded according to the pathology reports retrieved from the hospital information system. In tumors with both histopathological and cytological diagnosis, the histopathological diagnosis was taken into consideration.

MRI protocol

All images were acquired by using a 1.5 T MR system (Philips Achieva, Philips Medical Systems Nederland B.V.) with a superficial coil (Sense Flex-M coil). In the salivary gland MRI protocol - axial T_1W-TSE (T_1 weighted-turbo spin echo), axial T_2W-TSE (T_2 weighted-turbo spin eco), coronal STIR (short tau inversion recovery), axial DW-EPI (diffusion-weighted-echoplanar imaging) - were obtained. ADC maps were obtained from DWIs and the b values were selected as 0 and 800. After contrast medium administration, axial 12 dynamic T_1W-TSE with fat suppression and axial T_1W-TSE sequences were also obtained (Table 1). Non-specific gadolinium contrast medium 0.15 ml kg^{-1} was administered intravenously using an automatic injector (Medrad Spectris Solaris EP, Bayer Radiology Solutions) at 3 ml s^{-1}, followed by a flush of 25 ml of saline.

Table 1 MRI sequence characteristics in salivary gland protocol

	T_1W TSE	T_2W TSE-HR	STIR	T_1W TSE-HR	FS T_1W TSE	DW-EPI
FOV	200 × 218	210 × 210	200 × 220	210 × 210	200 × 200	225 × 225
Flip angle	90	90	90	90	10	90
TR	528	2515	6000	444	6,8	7170
TE	14	90	140	16	3,3	70
Slice	4	3	5	4	5	2
Matrix	224 × 196	264 × 204	232 × 185	244 × 195	168 × 166	112 × 112

DW-EPI, diffusion-weighted echoplanar imaging; FOV, field of view; FS, fat saturated; STIR, short tau inversion recovery; Slice, slice thickness; TE, echo time; TR, repetition time; T_1W TSE, T_1 weighted turbo spin echo.

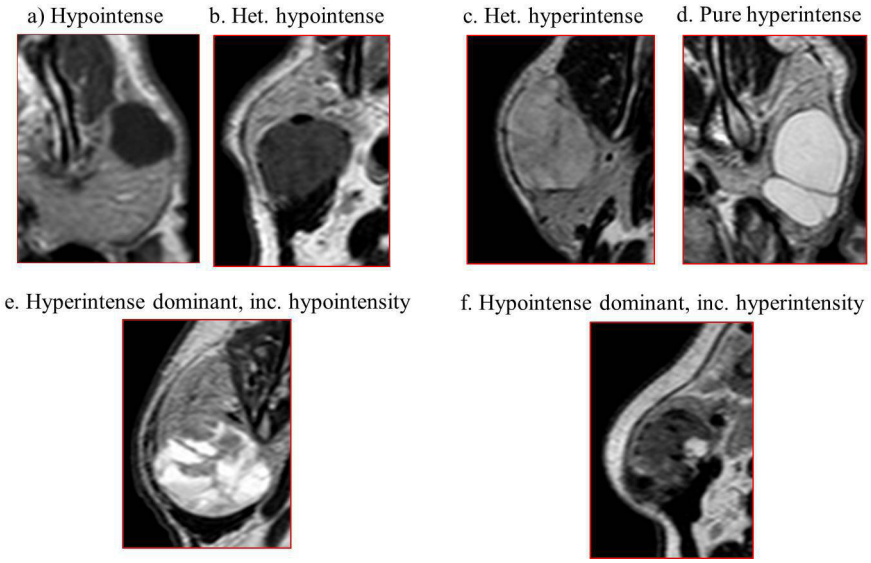

Figure 1 Case samples of subgroups created according to T_2W signal intensity characteristics in parotid gland tumors, (a) hypointense, (b) heterogeneous hypointense, (c) heterogeneous hyperintense, (d) pure hyperintense, (e) hyperintense dominant, including hypointensity, (f) hypointense dominant, including hyperintensity.

MRI analysis

Conventional MRI: All evaluations were made together with consensus by three radiologists. One of them had more than 25 years of experience in head and neck radiology; the other two had 4 years of general radiology experience. All researchers were blind to histopathological results. The location of the tumor (right, left, bilateral), size (the longest transverse diameter in the axial plan), contour (smooth, lobulated, irregular), border (well-circumscribed, irregular) and T_1W, T_2W signal intensity were recorded on conventional images. The increased signal intensity feature in T_2W images was divided into four subgroups to better identify common mixed masses (Type 1: hyperintense dominant, including hypointensity, Type 2: hypointense dominant, including hyperintensity, Type 3: pure hyperintense, Type 4: heterogeneous hyperintense) (Figure 1).

Apparent diffusion coefficient (ADC)

The ADC value was automatically calculated by drawing a manual region of interest (ROI) from a single section in the axial plan via the software program. Conventional sequences were examined prior to measurement. The periphery of the mass and necrotic components, if any, was avoided during measurement. Measurements were made from the widest plan covering the entire tumor. Mean, minimum and maximum ADC values were recorded on the automatically generated histogram analysis table. The relative ADC value is the ratio of the mean ADC value of the tumor to the mean ADC value measured from the normal parotid gland parenchyma (at least 1 cm away from the tumor or from the opposite parotid gland) (Figure 2).

Statistical analysis

Statistical analysis was performed using Statistical Package for Social Sciences v. 22.0 (IBM Corp.; Chicago, IL). All tumors were divided into two main groups, malignant and benign, and with subgroups within these two groups. Appropriation of mean, minimum, maximum and relative ADC values to normal distribution in all groups was investigated using the Kolmogorov–Smirnov test. Those that are suitable for normal distribution were recorded as "mean ± standard deviation" and those outside were "median (25th–75th percentile)". Statistical significance was investigated for all subgroups for T1 and T2 signal intensities and ADC (mean, minimum, maximum, relative) between benign–malignant tumors and the two most common benign tumors, pleomorphic adenoma–Warthin tumor. The optimal threshold value for differentiation was calculated using receiver operating characteristic (ROC) analysis. "Student's *t* Test" was used for normally distributed groups and "Mann–Whitney *U*" test was used for others. χ^2 test was used to evaluate the categorical data. The specificity, sensitivity, positive-predictive value (PPV) and negative-predictive value (NPV) of the optimal threshold value in groups were calculated. Findings with a p-value < 0,05 were considered significant.

Results

There were 60 tumors in 60 patients in the study group. 39 of them were male, 21 female. Mean age was 59 ± 14 years (age range 18–86 years). The maximum width of the lesions ranged between 11 and 61 mm, and the mean was 26 ± 10 mm.

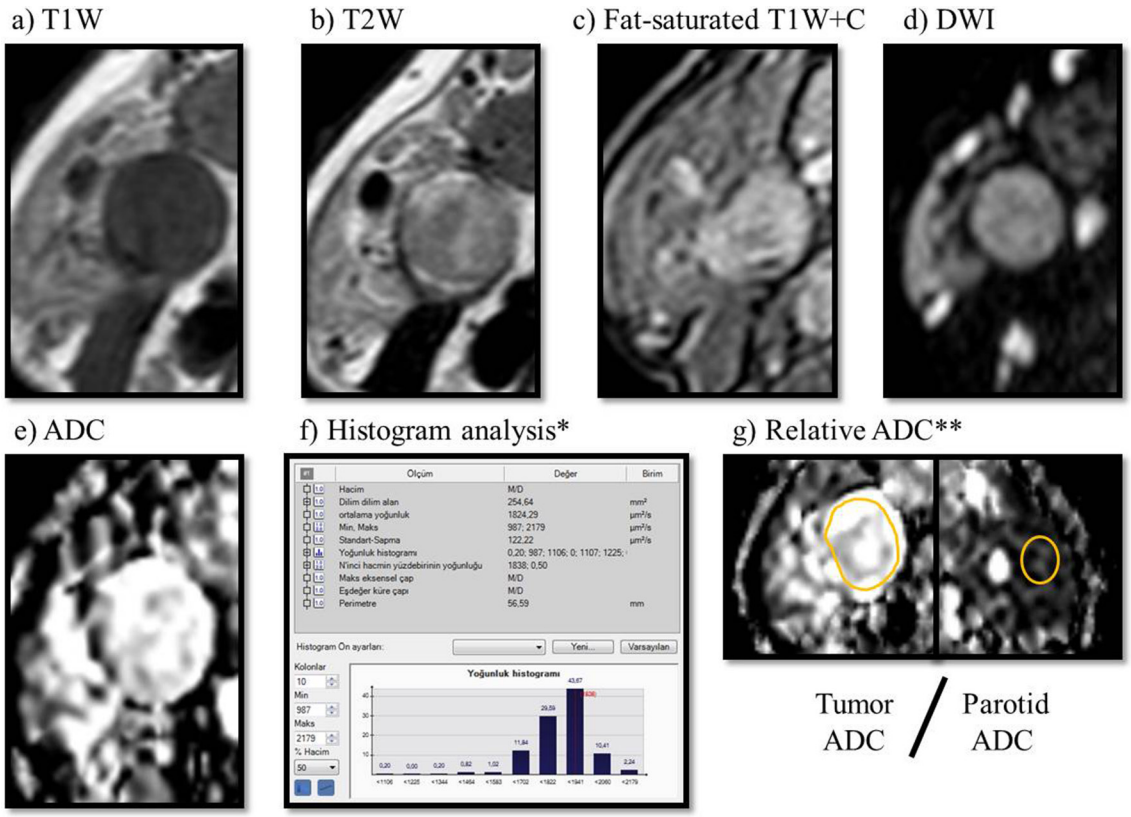

Figure 2 Warthin tumor in the right parotid gland, (a) T_1W, (b) T_2W, (c) post-contrast fat-saturated T_1W, (d) DWI, (e) ADC, (f) histogram analysis was obtained by drawing a manual ROI on the ADC map (f). Mean, minimum, maximum ADC value of tumor (g) Relative ADC: tumor ADC/Normal parotid gland ADC ratio. ADC, apparent diffusion coefficient, DWI, diffusion-weighted imaging.

The final diagnoses were obtained by histopathology in 38 patients and cytology in 22. 48 of 60 tumors were diagnosed as being benign and 12 (20%) malignant. Warthin tumor was the most frequent tumor in the series (n: 25, 42%), followed by pleomorphic adenoma (n: 15, 25%) were the most common benign tumors. Other benign tumors were basal cell adenoma (n: 1, 2%). Five tumors were diagnosed as benign on cytology. There were five squamous cell carcinomas (8%), four follicular cell lymphomas (7%) and three adenocarcinomas (6%) in the malignant group. 7 of the 60 tumors were bilateral.

The majority of tumors had a well-defined border (91%) and lobulated contour (62%) (Table 2).

All of the malignant tumors appeared hypointense on T_1 weighted images, and 41% were homogeneous and 41% were heterogeneous. Similarly, 81% of benign masses were hypointense on T_1 weighted images. When T1 signals were compared, no significant difference was found between malignant and benign tumors ($p = 0.266$). T2 signal was hyperintense in 80% of the masses. When T_2 weighted images were evaluated, 94% of benign lesions were hyperintense and 75% of malignant lesions were hypointense. There was a statistically significant difference between the groups ($p < 0.001$). Among the subgroups, "hyperintense dominant, including hypointensity" (35%) and hypointense dominant of T2 signal, "including hyperintensity" (28%) were more common. In 16 of 25 Warthin tumors, "hypointense dominant, including hyperintensity" T2 signal intensity characteristics were observed. All Warthin tumors with hyperintense T2 signal were found to be in the "hypointense dominant, including hyperintensity" subgroup. The T2 intensity type was "hyperintense dominant, including hypointensity" were detected in 13 of 15 of pleomorphic adenomas and there was also a statistically significant difference between benign masses for T_2 weighted hyperintensity subgroups ($p < 0.001$). (Table 3).

Mean, minimum, maximum and relative ADC values were calculated for all tumors. ADC values in all tumor groups are summarized in Table 4. The mean ADC value for benign tumors ($1.6 \pm 0.6 \times 10^{-3}$ mm^2 s^{-1}) was found to be higher than the malignant ones ($0.8 \pm 0.3 \times 10^{-3}$ mm^2 s^{-1}). There was statistically significant difference between benign–malignant tumor groups for all subgroups of ADC [ADCmean: (p: 0.0005), ADC minimum: (p: 0.013), ADC maximum: (p: 0.001), relative ADC: (p: 0.009), Student's t test)].

The ADC values of Warthin were lower than those of pleomorphic adenoma. These two benign tumors showed a statistically significant difference on behalf of all subgroups of ADC values [ADCmean: (p: 0.001), ADCminimum: (p: 0.002), ADC maximum: (p: 0.001),

Table 2 Demographic features and conventional MRI findings of tumor subgroups

Tumors		*Benign (n:48)*						*Malign (n:12)*			
		PA	*WA*	*BCA*	*Cyst*	*Lipoma*	*BC*	*Adeno*	*SCC*	*FL*	*Total*
Number of cases		15	25	1	1	1	5	3	5	4	60
Age[a]		55	57	52	34	77	70	60	64	70	59
Gender (M/F)		7/8	17/8	F	M	M	4/1	M	2/3	M	39/21
Size (mm)[a]		25	26	18	28	33	21	27	24	38	26
Location	Right	7 (%46)	7 (%28)	1	–	–	2 (%40)	3 (%100)	5 (%100)	1 (%25)	26 (%43)
	Left	8 (%54)	12 (%48)	–	1	1	3 (%60)	–	–	2 (%50)	27 (%45)
	Bilateral	–	6 (%24)	–	–	–	–	–	–	1 (%25)	7 (%12)
Contour	Smooth	6 (%40)	4 (%16)	–	–	–	4 (%80)	1 (%33)	1 (%20)	–	16 (%26)
	Lobulated	8 (%53)	19 (%76)	1	1	1	1 (%20)	–	3 (%60)	3 (%75)	37 (%62)
	Irregular	1 (%7)	2 (%8)	–	–	–	–	2 (%67)	1 (%20)	1 (%25)	7 (%12)
Border	Circumscribed	14 (%93)	24 (%96)	1	1	1	5 (%100)	1 (%33)	4 (%80)	3 (%75)	54 (%90)
	Irregular	1 (%7)	1 (%4)	–	–	–	–	2 (%67)	1 (%20)	1 (%25)	9 (%10)

Adeno, adenocarcinoma; BC, benign cytology; BCA, basal cell adenoma; Cyst, lymphoepithelial cyst; FL, follicular lymphoma; PA, pleomorphic adenoma; SCC, squamous cell carcinoma; WA, Warthin tumor.
[a]If the number of tumors is more than one, it is given as a mean.

ADC relative: (*p*: 0.001)/Mann–Whitney *U*). There was also significant difference between Warthin tumor in comparison to all malignant tumors for mean-maximum-relative ADC [ADCmean: (*p*: 0.015), ADC maximum: (*p*: 0.002), ADC relative: *p*: 0.025], and no difference was found for the minimum ADC value (*p*: 0,215, Mann–Whitney *U*). While there was statistically significant difference for mean-maximum-relative ADC between follicular lymphoma–other malignant tumors [ADCmean: (*p*: 0.025), ADC maximum: (*p*: 0.015), ADC relative: (*p*: 0.035), but no difference for the minimum ADC (*p*: 0,518, Mann-Whitney-U), (Table 4).

According to the ROC analysis, a threshold 1.2 × 10^{-3} mm^2 s^{-1} for the mean ADC value revealed a sensitivity of 100%, specificity: 71%, PPV: 46%, NPV: 100%, in differentiating malignant from benign. The 1.4 × 10^{-3} mm^2 s^{-1} threshold value showed a sensitivity of 100%, specificity: 70%, PPV: 65%, NPV: 100% in differentiating pleomorphic adenoma and Warthin tumor (Figure 3).

Discussion

Surgical resection is currently the best treatment for salivary gland tumors. It is favorable to define the tumor type precisely before surgery, in order to choose the surgical method and to predict possible complications. FNAC is accepted as the standard diagnostic method for parotid

Table 3 Conventional MRI, T1 and T2 characteristics of all tumor types

Tumors		*Benign (n:48)*						*Malign (n:12)*			
		PA	*WA*	*BCA*	*Cyst*	*Lipoma*	*BC*	*Adeno*	*SCC*	*FL*	*Total*
Number of cases		15	25	1	1	1	5	3	5	4	60
*T*1W	Pure hypointense	8 (%53)	8 (%32)	–	1	–	3 (%60)	2 (%67)	1 (%20)	3 (%75)	26 (%43)
	Pure hyperintense	1 (%7)	1 (%4)	–	–	1	–	–	–	–	3 (%5)
	Heterogeneous hypointense	4 (%27)	13 (%52)	1	–	–	1 (%20)	1 (%33)	4 (%80)	1 (%25)	25 (%42)
	Heterogeneous hyperintense	2 (%13)	2 (%8)	–	–	–	–	–	–	–	4 (%7)
	Isointense	–	1 (%4)	–	–	–	1 (%20)	–	–	–	2 (%3)
*T*2W	Pure hypointense	–	–	–	–	–	–	–	–	2 (%50)	2 (%3)
	Heterogeneous hypointense	1 (%7)	2 (%8)	–	–	–	–	2 (%67)	3 (%60)	2 (%50)	10 (%17)
	Isointense	–	–	–	–	–	–	–	–	–	–
Hyperintense[a]	Type 1	13 (%86)	7 (%28)	–	–	–	1 (%20)	–	–	–	21 (%35)
	Type 2	–	16 (%64)	–	–	–	1 (%20)	–	–	–	17 (%28)
	Type 3	1 (%7)	–	–	1	1	3 (%60)	–	–	–	6 (%10)
	Type 4	–	–	1	–	–	–	1 (%33)	2 (%40)	–	4 (%7)

Adeno, adenocarcinoma; BC, benign cytology; BCA, basal cell adenoma; Cyst, lymphoepithelial cyst; FL, follicular lymphoma; PA, pleomorphic adenoma; SCC, squamous cell carcinoma; WA, Warthin tumor.
[a]Increased signal intensity feature in T_2W images was divided into four subgroups; Type 1: hyperintense dominant, including hypointensity, Type 2: hypointense dominant, including hyperintensity, Type 3: pure hyperintense, Type 4: heterogeneous hyperintense.

Table 4 ADC values in tumor groups

		ADC ($x10^{-3}$ mm^{-2} s^{-1})			
Tumor types	*Number*	*Mean*	*Minimum*	*Maximum*	*Relative*
Benign	48	1,6 ± 0,6	0,5 (0,4–0,9)	2,4 ± 0,7	1,6 ± 0,6
Pleomorphic adenoma	15	1,9 ± 0,3	0,8 (0,5–0,9)	2,8 ± 0,6	1,9 ± 0,3
Warthin tumor	25	1 (0,9–1,8)	0,5 ± 0,3	2 ± 0,6	1,1 (0,9–1,8)
Lipoma	1	2,6	1,3	3,4	2
Lymphoepithelial cyst	1	2	1,5	2,5	2
Basal cell adenoma	1	1,4	0,7	1,8	1
Benign cytology	5	2 ± 0,6	0,8 ± 0,3	2,7 ± 0,6	2,3 ± 0,7
Malignant	12	0,8 ± 0,3	0,4 ± 0,1	1,5 ± 0,5	1 ± 0,6
Adenocarcinoma	3	0,9 (0,8–1,2)	0,5 (0,4–0,7)	1,5 (1,0–2,1)	0,9 (0,8–1)
Squamous cell carcinoma	5	0,8 (0,7–1,0)	0,3 (0,2–0,6)	1,6 (1,2–2)	1 (0,9–2)
Follicular lymphoma	4	0,6 (0,5–0,7)	0,3 (0,1–0,4)	1 (0,8–1,3)	0,5 (0,4–0,6)

ADC, apparent diffusion coefficient.
Number of lesions ≥ 5: If values fit for normal distribution: Mean ± std. if does not fit: Median (25th–75th percentile).
+ 2 <Number of lesions <5: Median (minimum–maximum).
+ Number of lesions = 1: Only measured value.

gland masses.[4,14] Although FNAC has a high diagnostic accuracy in the hands of experienced cytologists, it is often difficult to differentiate parotid tumors with multivariate histology.[15,16] Relatively invasive and expensive techniques such as ultrasound guided tru-cut biopsy and intraoperative biopsy had been proposed for being higher diagnostic accuracy.[17,18]

In recent years, MRI has been proposed as a non-invasive diagnostic tool that may obviate the need for FNAC.[19] Fassnacht et al[20] reported a sensitivity of 45%, specificity 89%, and accuracy 84% in predicting malignancy for FNAC. These values were 40, 88, and 81% For MR, respectively. The cumulative sensitivity of MRI and FNAC was 50%, specificity 85% and accuracy %80. Furthermore, MRI together with DWI showed a better success rate with a sensitivity of 70%, specificity and accuracy 91%.[20]

MRI has been accepted to be the most sensitive and specific imaging test to determine the type, location, spread, and relationship with adjacent soft tissues of parotid tumors.[21] Irregular border, extraglandular extension, and accompanying enlarged lymph node were proposed as signs for malignancy, which can be easily evaluated by conventional MRI.[3,22,23] Although T2 hypointensity and inhomogeneity may suggest malignant tumors, it is not adequate enough for the differentiation.[24] Although benign masses tend to have relatively homogeneous signal intensity, hemorrhage and calcification may cause a heterogeneous appearance mimicking malignancy.[3] In our study, only 33%

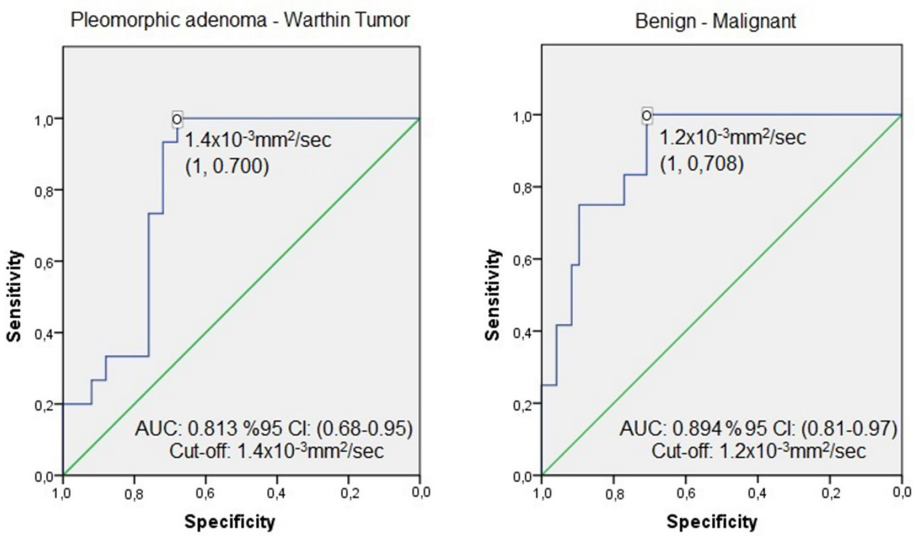

Figure 3 ROC curves in selected tumor groups. AUC, area under the curve; ROC, receiver operating characteristic.

of the malignant tumors showed irregular margins and 58% appeared hypointense and heterogeneous in T_2W images. In result, malign–benign distinction may barely rely on morphological characteristics neither irregular margins nor heterogeneous/hypointense on T2 alone.

Intravenous administration of contrast material, better with dynamic techniques, has been shown to enhance the diagnostic performance of MRI. However, the use of gadolinium chelates in under debate for the side-effects like accumulation in tissues of the body. In addition to the increase in costs and other known side-effects, intravenous gadolinium chelates causes nephrogenic systemic fibrosis as a serious side-effect in patients with renal failure.[25–27] These reasons brought the need to develop MR techniques that can be performed without using intravenous gadolinium.

As a functional imaging method DWI that complements routine MRI, has increased its importance in recent years by providing both qualitative and quantitative data, and may preclude the need for contrast agents. Yuan et al[28] has compared the diagnostic efficacy of conventional MRI, dynamic contrast-enhanced MRI and DWI in the differentiation of benign–malignant parotid tumors in a study of 207 cases. They reached to a conclusion that the post-contrast images did not improve the value of conventional MRI, while DWI had a positive impact on the diagnostic efficiency. In our study, although there were contrast enhanced series, they were not taken under consideration due to the difference in the techniques used for contrast administration. Hence, our study was based on the morphologic analysis and DWI alone.

Salivary gland tumors are rare. Most of the tumors are benign. The most common benign tumors are pleomorphic adenoma and Warthin tumor.[2,29] The possibility of the existing tumor to be one of these two histopathological types should be considered first. Pleomorphic adenoma is seen as a well-circumscribed, smooth or slightly lobulated contour, encapsulated mass, containing myxoid, mucoid or chondroid areas within the epithelial tissue, microscopically. The myxoid stroma provides the characteristic T2 hyperintense signal, while the epithelial component is seen as T2 hypointense. Warthin tumor, on the other hand, is a well-circumscribed, lobulated contour, non-encapsulated mass. On microscopy, epithelial tissue with lymphoid hyperplasia, and a variable size cystic component containing approximately 30% proteinous fluid or viscous colloid. Although this tumor frequently appears hypointense in T_2W images, it can also contain hyperintensities if cystic component exist.[30–32] There are studies that rely on the T_2W signal intensity characteristics to discriminate these two, most frequently encountered benign tumors. In a quantitative study by Eiji et al[33] it was shown that T_2W intensity in pleomorphic adenoma was significantly higher than Warthin tumor and malignant tumors. Tsushima et al[32] reported a high probability for pleomorphic adenoma when the mass appeared brighter than the cerebrospinal fluid signal on T2. Benign lesions of the parotid gland may contain a varying amount of dark and bright areas on T_2W sequence, which is formed as a reflection of its histopathological structures. It was the reason why we tried to focus on the radiological morphology of the tumors on T_2W series, and group them according to the signal intensity dominance. In our study, 13 of 15 pleomorphic adenomas had Type 1 and, 16 of 25 Warthin tumors had Type 2 (Table 3). We could not come across a similar classification in the related literature, but came to a conclusion that the T2 hyperintense dominant signal might primarily suggest pleomorphic adenoma among masses with heterogeneous appearance. However, 9 of 25 Warthin tumors were misdiagnosed as pleomorphic adenoma and 2 as malignant tumor. This might be explained by the amount of cystic component that can be encountered in Warthin tumor. As the size of cystic component increases, the internal structure looks bright on T_2W images that may simulate pleomorphic adenoma (Figure 4). Conversely as the cystic component gets smaller, the T2 signal of Warthin tumor gets darker very similar with malignant tumors. The T_2W signal of 7 of the 9 malignant tumors in our series were categorized as hypointense/heterogeneous or hypointense (78%). By the way, in the absence of other well-known features of malignancy, like irregular contour or blurred margins, the T_2W signal properties alone may cause some misdiagnosis.

The additive role of DWI to conventional MRI in the differentiation of benign and malignant masses and the histopathological types has been explored in recent years. DWI uses regional differences in the movement of water molecules within the extracellular/extravascular compartments of biological tissues. When the compact structure of the extracellular space, such as with lymphoma, carcinoma and abscess, causes the barrier effect in the movement of the water molecules, water diffusion is said to be "restricted" in these tissues. Conversely, in necrotic or fluid-filled (cysts) tissues that are said to be "free", there is unlimited movement of water molecules. Therefore, DWI gives information about diffusion properties in different tissues, cellularity and cellular membrane features.[34,35] ADC that is obtained from DWI provides quantitative data about the water diffusion properties of tissue. ADC gives the absolute value of the magnitude of the measured diffusion and is independent from diffusion direction and T2 effect. Many studies have shown that benign tumors have higher ADC values than malignant tumors.[8,10,11,19,36,37] Different mean ADC values have been reported in the relevant literature, beyond this disagreement ADC was found to be beneficial in differentiating benign and -malignant tumors. In contrast, Matsushima et al[38] found the mean ADC value of $1.09 \pm 0.34 \times 10^{-3}$ mm^2 s^{-1} in malignant tumors, and $1.40 \pm 0.43 \times 10^{-3}$ mm^2 s^{-1} for benign tumors and there was no statistical significance ($p > 0.05$). They concluded that the ADC value increased with the increase of extracellular components,

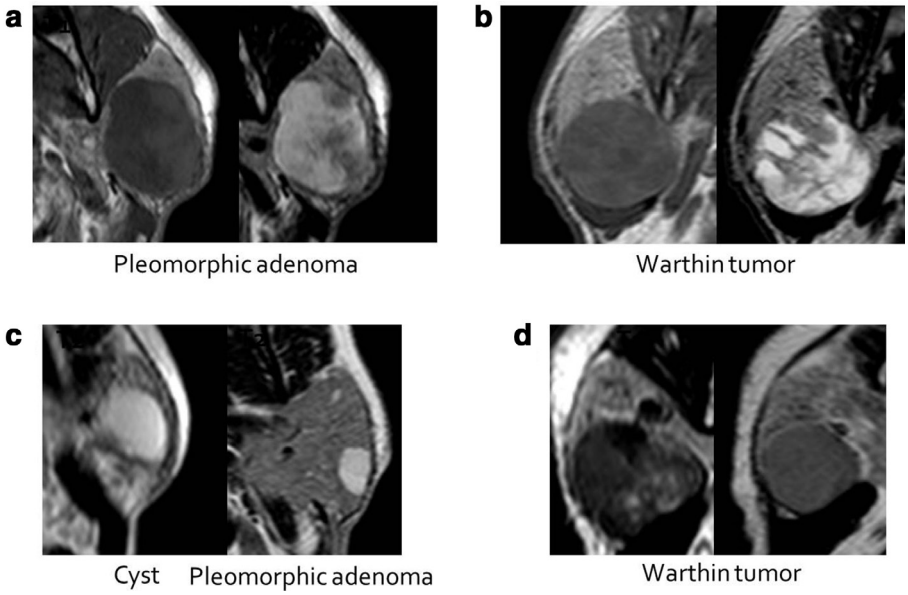

Figure 4 MRI signal characteristics of pleomorphic adenoma and Warthin tumor; (a) PA: T1 heterogeneous hypointense, mixed signal containing T2 hyperintense dominant, including hypointensity. Typical appearance with cystic dominant nodular/septal component. (b) Warthin tumor: Mixed signal containing T1 heterogeneous hypointense, T2 hyperintense dominant, including hypointensity. When Warthin tumor's cystic component size increases, imaging features show similarity with PA. (c) lymphoepithelial cyst and pleomorphic adenoma cases: in small PA's, nodular/septated component cannot be clearly seen in some cases. (d) Two different Warthin tumor cases: The size of the cystic components in Warthin tumors is variable. If the size is small, it is difficult to distinguish it from malignant tumors. PA, pleomorphic adenoma.

and therefore the ADC value alone was not sufficient to differentiate benign from malignant.[38] In Habermann et al.'s study in 2009, the ADC value was found to be significantly higher in pleomorphic adenomas than other tumors ($2.09 \pm 0.16 \times 10^{-3}$ mm^2 sec^{-1}, p: 0.054). However, they could not detect a significant difference between benign-malignant tumors.[14] Çelebi et al[39] investigated the usefulness of quantitative analysis with ADC measurement in parotid gland tumors and determined the threshold value of $1{,}165 \times 10^{-3}$ mm^2 s^{-1} to distinguish benign and malignant masses in 2013, which was very similar value of our study. Also they reported a sensitivity of 63%, specificity 72%, PPD 79% and NPD 79% for this threshold value.[39] Tissue microstructure, cellularity, tumor types or device dependent factors like screening protocol (b value) and measurement technique may explain the difference of ADC values between studies. Although diagnostic success was higher than the previously discussed studies, PPV was lower. The reason for this might be the very low ADC value of Warthin tumor in regard to other benign tumors. Also, the relatively high number of Warthin tumors in our study group compared to other studies. In 14 of 25 Warthin tumors, the ADC value was lower than the threshold in our study. On the other hand, this value was still higher than malignant tumors (p: 0.015). One-third of the malignant cases in our study were lymphomas. It is known that lymphomas show a lower ADC value compared to other common malignancies.[40] In this study, lower ADC values were found in lymphoma cases compared to other malignant masses. This may have further reduced the mean ADC value of the malignant tumor and sharpened the sensitivity.

Studies have shown that ADC values are important and usable in the diagnosis of pleomorphic adenoma. In literature, there are many studies especially examining the ADC values of pleomorphic adenoma and Warthin tumor, which were reported to be useful.[4,38,41,42] We had similar results with the literature. When using the mean ADC threshold value of 1.4×10^{-3} mm^2 s^{-1} to differentiate these two benign masses, the sensitivity, specificity, PPV and NPV was found as 100, 70, 65, and 100%, respectively.

A recent study on diffusion tensor imaging showed near similar results by using fractional anisotropy value and mean diffusivity value equivalent to ADC value in DWI. They concluded that these two values could differentiate malignant from benign tumors and Warthin tumors from pleomorphic adenomas. Fractional anisotropy alone was stated to differentiate Warthin tumors from malignant salivary gland tumors.[43]

It is the "mean ADC" value that was in majority of in the related literature. Other ADC parameters are the minimum, maximum and relative ADC. The minimum ADC value represents the most proliferative area with the highest cellularity in heterogeneous tumors. In contrast, the maximum ADC indicates the area with the lowest cellularity and the highest extracellular fluid. There are studies in the literature showing that minimum ADC in breast and brain tumors is successful parameters in benign–malignant differentiation and tumor grading.[44,45] Relative ADC value was defined

to optimize the ADC value, which was calculated by dividing ADC value of the lesion by the adjacent gland parenchyma. Different from the other studies, we also evaluated minimum, maximum and relative ADC values in this cohort, but no significant advantages were found on mean ADC values.

The retrospective design and limited number of malignant cases were the major limitations of our study. Furthermore, DWI used has several limitations, mostly due to the sequence being obtained by EPI method.[46,47] SE-EPI provides limited image quality with low spatial resolution and poor SNR (signal-to-noise ratio) and is sensitive to blurring and ghosting artifacts. Also, the repeatability of quantitative ADC values has been questioned. It should also be noted that ADC values could vary significantly depending on hardware, human or biological factors. It will be beneficial to increase and confirm the existing knowledge with the studies to be performed with more cases.[48]

Conclusion

Prediction of tumor subtypes with imaging findings may contribute to future surgical practice. In this cohort, we used two basic, non-invasive and mostly accessible techniques, conventional MR and DWI. A thorough analysis of the T2 signal and ADC values may help to determine the nature of the tumors. The T2 signal alone may be useful in recognizing the pleomorphic adenoma and then Warthin tumors. Together with powerful supportive imaging findings for malignancy, T_2W hypointensity may support the diagnosis. But beyond all this, DWI draws interest with its non-invasive and non-contrast nature, and it increases the diagnostic performance when added to the conventional MRI protocol.

REFERENCES

1. Seifert G. *Histoligical typing of salivary gland tumors*. **15**. Berlin: Springer-Verlag; 1991. pp. 17.
2. Pinkston JA, Cole P. Incidence rates of salivary gland tumors: results from a population-based study. *Otolaryngol Head Neck Surg* 1999; **120**: 834–40. doi: https://doi.org/10.1016/S0194-5998(99)70323-2
3. Lee YYP, Wong KT, King AD, Ahuja AT. Imaging of salivary gland tumours. *Eur J Radiol* 2008; **66**: 419–36. doi: https://doi.org/10.1016/j.ejrad.2008.01.027
4. Boccato P, Altavilla G, Blandamura S. Fine needle aspiration biopsy of salivary gland lesions. A reappraisal of pitfalls and problems. *Acta Cytol* 1998; **42**: 888–98. doi: https://doi.org/10.1159/000331964
5. Das DK, Petkar MA, Al-Mane NM, Sheikh ZA, Mallik MK, Anim JT, et al. Role of fine needle aspiration cytology in the diagnosis of swellings in the salivary gland regions: a study of 712 cases. *Med Princ Pract* 2004; **13**: 95–106. doi: https://doi.org/10.1159/000075637
6. Behzatoğlu K, Bahadir B, Kaplan HH, Yücel Z, Durak H, Bozkurt ER, et al. Fine needle aspiration biopsy of the parotid gland. diagnostic problems and 2 uncommon cases. *Acta Cytol* 2004; **48**: 149–54. doi: https://doi.org/10.1159/000326308
7. Freling NJ, Molenaar WM, Vermey A, Mooyaart EL, Panders AK, Annyas AA, et al. Malignant parotid tumors: clinical use of Mr imaging and histologic correlation. *Radiology* 1992; **185**: 691–6. doi: https://doi.org/10.1148/radiology.185.3.1438746
8. Eida S, Sumi M, Sakihama N, Takahashi H, Nakamura T. Apparent diffusion coefficient mapping of salivary gland tumors: prediction of the benignancy and malignancy. *AJNR Am J Neuroradiol* 2007; **28**: 116–21PMID.
9. Habermann CR, Gossrau P, Graessner J, Arndt C, Cramer MC, Reitmeier F, et al. Diffusion-Weighted echo-planar MRI: a valuable tool for differentiating primary parotid gland tumors? *Rofo* 2005; **177**: 940–5. doi: https://doi.org/10.1055/s-2005-858297
10. Yoshino N, Yamada I, Ohbayashi N, Honda E, Ida M, Kurabayashi T, et al. Salivary glands and lesions: evaluation of apparent diffusion coefficients with split-echo diffusion-weighted MR imaging--initial results. *Radiology* 2001; **221**: 837–42. doi: https://doi.org/10.1148/radiol.2213010131
11. Motoori K, Yamamoto S, Ueda T, Nakano K, Muto T, Nagai Y, et al. Inter- and intratumoral variability in magnetic resonance imaging of pleomorphic adenoma: an attempt to interpret the variable magnetic resonance findings. *J Comput Assist Tomogr* 2004; **28**: 233–46. doi: https://doi.org/10.1097/00004728-200403000-00014
12. Abdel Razek AAK, Elkhamary SM, Nada N. Correlation of apparent diffusion coefficient with histopathological parameters of salivary gland cancer. *Int J Oral Maxillofac Surg* 2019; **48**: 995–1000. doi: https://doi.org/10.1016/j.ijom.2019.03.897
13. Abdel Razek AAK, Mukherji SK. State-Of-The-Art imaging of salivary gland tumors. *Neuroimaging Clin N Am* 2018; **28**: 303–17. doi: https://doi.org/10.1016/j.nic.2018.01.009
14. Habermann CR, Arndt C, Graessner J, Diestel L, Petersen KU, Reitmeier F, et al. Diffusion-Weighted echo-planar MR imaging of primary parotid gland tumors: is a prediction of different histologic subtypes possible? *AJNR Am J Neuroradiol* 2009; **30**: 591–6. doi: https://doi.org/10.3174/ajnr.A1412
15. Stewart CJ, MacKenzie K, McGarry GW, Mowat A. Fine-Needle aspiration cytology of salivary gland: a review of 341 cases. *Diagn Cytopathol* 2000; **22**: 139–46. doi: https://doi.org/10.1002/(SICI)1097-0339(20000301)22:3<139::AID-DC2>3.0.CO;2-A
16. Klijanienko J, Vielh P. Fine-needle sampling of salivary gland lesions. IV. review of 50 cases of mucoepidermoid carcinoma with histologic correlation. *Diagn Cytopathol* 1997; **17**: 92–8. doi: https://doi.org/10.1002/(SICI)1097-0339(199708)17:2<92::AID-DC3>3.0.CO;2-Q
17. Haldar S, Mandalia U, Skelton E, Chow V, Turner SS, Ramesar K, et al. Diagnostic investigation of parotid neoplasms: a 16-year experience of freehand fine needle aspiration cytology and ultrasound-guided core needle biopsy. *Int J Oral Maxillofac Surg* 2015; **44**: 151–7. doi: https://doi.org/10.1016/j.ijom.2014.09.025
18. Howlett DC, Skelton E, Moody AB. Establishing an accurate diagnosis of a parotid lump: evaluation of the current biopsy methods - fine needle aspiration cytology, ultrasound-guided core biopsy, and intraoperative frozen section. *Br J Oral Maxillofac Surg* 2015; **53**: 580–3. doi: https://doi.org/10.1016/j.bjoms.2015.03.015
19. Yerli H, Aydin E, Haberal N, Harman A, Kaskati T, Alibek S, et al. Diagnosing common parotid tumours with magnetic resonance imaging including diffusion-weighted imaging vs fine-needle aspiration cytology: a comparative study. *Dentomaxillofac Radiol* 2010; **39**: 349–55. doi: https://doi.org/10.1259/dmfr/15047967
20. Fassnacht W, Schmitz S, Weynand B, Marbaix E, Duprez T, Hamoir M, et al. Pitfalls in preoperative work-up of parotid gland tumours: 10-year series. *B-ENT* 2013; **9**: 83–8PMID.

21. Koyuncu M, ŞeŞen T, Akan HÜseyin, Ismailoglu AA, Tanyeri YÜcel, Tekat A, Şeşen T, Akan H, et al. Comparison of computed tomography and magnetic resonance imaging in the diagnosis of parotid tumors. *Otolaryngology–Head and Neck Surgery* 2003; **129**: 726–32. doi: https://doi.org/10.1016/j.otohns.2003.07.009
22. Christe A, Waldherr C, Hallett R, Zbaeren P, Thoeny H. Mr imaging of parotid tumors: typical lesion characteristics in MR imaging improve discrimination between benign and malignant disease. *AJNR Am J Neuroradiol* 2011; **32**: 1202–7. doi: https://doi.org/10.3174/ajnr.A2520
23. Som PM, Biller HF. High-grade malignancies of the parotid gland: identification with MR imaging. *Radiology* 1989; **173**: 823–6. doi: https://doi.org/10.1148/radiology.173.3.2813793
24. Teresi LM, Lufkin RB, Wortham DG, Abemayor E, Hanafee WN. Parotid masses: MR imaging. *Radiology* 1987; **163**: 405–9. doi: https://doi.org/10.1148/radiology.163.2.3562818
25. Gandhi SN, Brown MA, Wong JG, Aguirre DA, Sirlin CB. MR contrast agents for liver imaging: what, when, how. *Radiographics* 2006; **26**: 1621–36. doi: https://doi.org/10.1148/rg.266065014
26. Juluru K, Vogel-Claussen J, Macura KJ, Kamel IR, Steever A, Bluemke DA, et al. Quality imaging in patients at risk for developing nephrogenic systemic fibrosis: protocols, practices, and imaging techniques to maximize patient safety. *Radiographics* 2009; **29**: 9–22. doi: https://doi.org/10.1148/rg.291085072
27. American College of Radiology.ACR manual on contrast media. 2020. Available from: https://www.acr.org/-/media/ACR/Files/Clinical-Resources/Contrast_Media.pdf.
28. Yuan Y, Tang W, Tao X. Parotid gland lesions: separate and combined diagnostic value of conventional MRI, diffusion-weighted imaging and dynamic contrast-enhanced MRI. *Br J Radiol* 2016; **89**: 20150912. doi: https://doi.org/10.1259/bjr.20150912
29. Araya J, Martinez R, Niklander S, Marshall M, Esguep A. Incidence and prevalence of salivary gland tumours in Valparaiso, Chile. *Med Oral Patol Oral Cir Bucal* 2015; **20**: e532: e532: 9. doi: https://doi.org/10.4317/medoral.20337
30. Batsakis JG. *Tumors of the head and neck: clinical and pathological considerations*. 2nd Edition. Baltimore, MD.: Williams & Wilkins Co.; 1979.
31. Ikeda K, Katoh T, Ha-Kawa SK, Iwai H, Yamashita T, Tanaka Y, et al. The usefulness of Mr in establishing the diagnosis of parotid pleomorphic adenoma. *AJNR Am J Neuroradiol* 1996; **17**: 555–9.
32. Tsushima Y, Matsumoto M, Endo K, Aihara T, Nakajima T. Characteristic bright signal of parotid pleomorphic adenomas on T2-weighted Mr images with pathological correlation. *Clin Radiol* 1994; **49**: 485–9. doi: https://doi.org/10.1016/S0009-9260(05)81748-9
33. Matsusue E, Fujihara Y, Matsuda E, Tokuyasu Y, Nakamoto S, Nakamura K, et al. Differentiating parotid tumors by quantitative signal intensity evaluation on MR imaging. *Clin Imaging* 2017; **46**: 37–43. doi: https://doi.org/10.1016/j.clinimag.2017.06.009
34. Taouli B, Koh D-M. Diffusion-Weighted MR imaging of the liver. *Radiology* 2010; **254**: 47–66. doi: https://doi.org/10.1148/radiol.09090021
35. Bammer R. Basic principles of diffusion-weighted imaging. *Eur J Radiol* 2003; **45**: 169–84. doi: https://doi.org/10.1016/S0720-048X(02)00303-0
36. Lyng H, Haraldseth O, Rofstad EK. Measurement of cell density and necrotic fraction in human melanoma xenografts by diffusion weighted magnetic resonance imaging. *Magn Reson Med* 2000; **43**: 828–36. doi: https://doi.org/10.1002/1522-2594(200006)43:6<828::AID-MRM8>3.0.CO;2-P
37. Wang J, Takashima S, Takayama F, Kawakami S, Saito A, Matsushita T, et al. Head and neck lesions: characterization with diffusion-weighted echo-planar MR imaging. *Radiology* 2001; **220**: 621–30. doi: https://doi.org/10.1148/radiol.2202010063
38. Matsushima N, Maeda M, Takamura M, Takeda K. Apparent diffusion coefficients of benign and malignant salivary gland tumors. Comparison to histopathological findings. *J Neuroradiol* 2007; **34**: 183–9. doi: https://doi.org/10.1016/j.neurad.2007.04.002
39. Celebi I, Mahmutoglu AS, Ucgul A, Ulusay SM, Basak T, Basak M, et al. Quantitative diffusion-weighted magnetic resonance imaging in the evaluation of parotid gland masses: a study with histopathological correlation. *Clin Imaging* 2013; **37**: 232–8. doi: https://doi.org/10.1016/j.clinimag.2012.04.025
40. Vidiri A, Minosse S, Piludu F, Pellini R, Cristalli G, Kayal R, et al. Cervical lymphadenopathy: can the histogram analysis of apparent diffusion coefficient help to differentiate between lymphoma and squamous cell carcinoma in patients with unknown clinical primary tumor? *Radiol Med* 2019; **124**: 19–26. doi: https://doi.org/10.1007/s11547-018-0940-1
41. Fruehwald-Pallamar J, Czerny C, Holzer-Fruehwald L, Nemec SF, Mueller-Mang C, Weber M, et al. Texture-based and diffusion-weighted discrimination of parotid gland lesions on Mr images at 3.0 Tesla. *NMR Biomed* 2013; **26**: 1372–9. doi: https://doi.org/10.1002/nbm.2962
42. Yabuuchi H, Matsuo Y, Kamitani T, Setoguchi T, Okafuji T, Soeda H, et al. Parotid gland tumors: can addition of diffusion-weighted MR imaging to dynamic contrast-enhanced MR imaging improve diagnostic accuracy in characterization? *Radiology* 2008; **249**: 909–16. doi: https://doi.org/10.1148/radiol.2493072045
43. Khalek Abdel Razek AA. Characterization of salivary gland tumours with diffusion tensor imaging. *Dentomaxillofac Radiol* 2018; **47**: 20170343. doi: https://doi.org/10.1259/dmfr.20170343
44. Hirano M, Satake H, Ishigaki S, Ikeda M, Kawai H, Naganawa S, et al. Diffusion-Weighted imaging of breast masses: comparison of diagnostic performance using various apparent diffusion coefficient parameters. *AJR Am J Roentgenol* 2012; **198**: 717–22. doi: https://doi.org/10.2214/AJR.11.7093
45. Kitis O, Altay H, Calli C, Yunten N, Akalin T, Yurtseven T, et al. Minimum apparent diffusion coefficients in the evaluation of brain tumors. *Eur J Radiol* 2005; **55**: 393–400. doi: https://doi.org/10.1016/j.ejrad.2005.02.004
46. Koh D-M, Collins DJ. Diffusion-Weighted MRI in the body: applications and challenges in oncology. *AJR Am J Roentgenol* 2007; **188**: 1622–35. doi: https://doi.org/10.2214/AJR.06.1403
47. Baliyan V, Das CJ, Sharma S, Gupta AK. Diffusion-Weighted imaging in urinary tract lesions. *Clin Radiol* 2014; **69**: 773–82. doi: https://doi.org/10.1016/j.crad.2014.01.011
48. Sasaki M, Yamada K, Watanabe Y, Matsui M, Ida M, Fujiwara S, et al. Variability in absolute apparent diffusion coefficient values across different platforms may be substantial: a multivendor, multi-institutional comparison study. *Radiology* 2008; **249**: 624–30. doi: https://doi.org/10.1148/radiol.2492071681